J Mater Sci (2012) 47:1436–1445
DOI 10.1007/s10853-011-5924-7

Well-organized 3D urchin-like hierarchical TiO_2 microspheres with high photocatalytic activity

Liqin Xiang · Xiaopeng Zhao · Jianbo Yin · Baolin Fan

Received: 6 June 2011 / Accepted: 30 August 2011 / Published online: 16 September 2011

Abstract This article reported a well-organized 3D urchin-like hierarchical TiO_2 which was synthesized by a simple solvothermal method without using any template or surfactant. The results of scanning electron microscopy, transmission electron microscopy, energy-dispersive X-ray spectroscopy, and powder X-ray diffraction showed that the hierarchical morphology and size of TiO_2 could be effectively controlled by adjusting the precursor ratio of tetrabutyl titanate to $TiCl_4$ solution, the concentration of $TiCl_4$ solution, the solvothermal temperature, and the reaction time. It is believed that the formation of the urchin-like hierarchical TiO_2 followed a 'nucleation–self-assembly–dissolution-recrystallization' growth mechanism. In addition, the excellent photocatalytic activity of the urchin-like hierarchical TiO_2 was confirmed by photodegradation of methyl blue in water.

Introduction

TiO_2 is one of most important functional materials due to its outstanding properties such as high photocatalytic activity, biological and chemical inertness, long term stability, low cost, non-toxicity, and so on [1, 2]. TiO_2 and its composites have been explored adequately in many fields including photocatalyst [1, 3–5], solar cell [6], antibacterial agent [7], electrorheology [8–10], and so on. In particular, TiO_2 has been accepted as one of the most important candidates for photodegradation of organic pollutants. It is evident that the size, morphology, and crystallinity of TiO_2 are important for its properties and applications [1, 11–14].

L. Xiang · X. Zhao (✉) · J. Yin · B. Fan
Smart Materials Laboratory, Department of Applied Physics, Northwestern Polytechnical University, Xi'an 710072, China
e-mail: xpzhao@nwpu.edu.cn

In the past decades, the nanosized TiO_2 has attracted considerable attention due to enhanced photocatalytic activity. The nanosized TiO_2 with different morphology, such as spheres [15], hollow spheres [16], nanotubes [17–19], nanoneedles [20], and mesoporous film [21, 22] has been successfully prepared by various techniques. However, the difficulty of separation of suspended nanosized TiO_2 from water inevitably limits the application of nanosize TiO_2 especially in the waste-water treatment field [23]. One of the strategies to overcome this obstacle is to design and prepare 3D micro/nanohierarchical materials [24–27]. The multilevel interior structure such as hierarchically porous particles and epitaxial multilevel structure such as urchin-like microspheres are two types of typical miro/nano hierarchical structure [24, 28]. The template-induced self-assembly method is the main approach to prepare the hierarchical materials. However, the utilization and removal of templates easily introduce impurities into products. The template-free self-assembly method is considered to be an ideal strategy. Recently, various hierarchical TiO_2 has been prepared by the template-free self-assembly method under different conditions. For example, Wang et al. [29] synthesized anatase TiO_2 3D hierarchical nanostructures by a hydrothermal method. Gao's group prepared urchin-like TiO_2 with a diameter about 1 μm via a sol-solvothermal process based on benzene-water interfaces [30]. Li et al. [31] successfully synthesized hollow TiO_2 spheres with urchin-like morphology. Cheng et al. [32] further investigated electrorheological characteristics of sea-urchin-like TiO_2 hollow spheres. Mao et al. [33] synthesized hollow TiO_2 spheres with sea-urchin-like structures by H_2O_2-assisted hydrothermal method. Zhang et al. [34] prepared TiO_2 with 3D hierarchical architectures by the microwave-assisted hydrothermal method. Furthermore, other flower-like TiO_2 and urchin-like TiO_2 were

also synthesized by different techniques [35–38]. However, the formation mechanism of self-assemble hierarchical TiO_2 has not been well understood and some synthetic strategies depend on the experience of researchers [24]. Obviously, it is still a challenge to well control the size and morphology of hierarchical TiO_2 simultaneity. Furthermore, the properties of hierarchical metal oxide are attracting more and more attention [35–38].

In the previous work, our group has confirmed that the rheological property of urchin-like TiO_2 particle suspension was significantly different from that of smooth particle suspension [27]. In this article, we take special note of the formation mechanism of the urchin-like hierarchical TiO_2 microsphere and study its photocatalytic activity. The influences of different reaction conditions including the ratio of reactants, reaction time, reaction temperature, and concentration of reactants on the morphology and size of hierarchical microsphere were investigated systematically. A new formation mechanism of the hierarchical urchin-like structure was proposed based on the experimental results. The excellent photocatalytic activity of the urchin-like hierarchical TiO_2 microsphere was confirmed by photodegradation of methyl blue (MB) in water. The results may be useful to the deeper comprehension of the formation mechanism of micro/nanohierarchical TiO_2. It is also favorable to explore effective and economical methods for preparation of hierarchical TiO_2 microspheres with high photocatalytic activity.

Experimental procedure

Preparation

All chemicals were of analytical grade and used as-received. Initially, titanium tetrachloride ($TiCl_4$, Kermel Chemical Reagent Co. Ltd of China) was dissolved into distilled water in an ice-water bath under vigorous stirring to obtain a 50 wt% $TiCl_4$ aqueous solution. Then, 4 mL of tetrabutyl titanate (TBT, Kermel Chemical Reagent Co. Ltd of China) was dissolved in 30 mL of toluene in an ice-water bath and subsequently 4 mL of $TiCl_4$ aqueous solution was added dropwise into the TBT/toluene solution under stirring. After further stirring for 1 h, the mixture was transferred into a 50 mL stainless steel autoclave lined with Teflon and held at 150 °C for 24 h. Finally, the precipitates were filtered, washed with ethanol for several times, and dried at 70 °C to obtain the product.

To investigate the influences of different reaction conditions and understand the formation mechanism of the hierarchical TiO_2, the ratio of reactants, reaction time, temperature, and concentration of the reactant in synthesis were changed.

Characterization

The size and morphology of samples were observed by scanning electron microscopy (SEM, JSM-6700) and transmission electron microscopy (TEM, JEOL-3010). The chemical composition of samples was analyzed by energy-dispersive X-ray spectroscopy (TEM/EDS, JEOL-3010). The crystal structure of samples was characterized by the powder X-ray diffraction (XRD) patterns at a Philips X'Pert Pro X-ray diffractometer with Cu K_α irradiation (40 kV/35 mA) and step size of 0.033° in the 2θ range of 10°–70°. The nitrogen adsorption isotherms and special surface areas were determined by a Quantachrome Nova2000e surface area and pore size analyzer. All samples were degassed at 150 °C under a vacuum for a minimum of 6 h. The special surface areas were calculated using the Brunauer–Emmett–Teller (BET) model from a linear part of the BET plot (P/P_0) 0.10–0.30).

Photocatalytic test

Analytical grade basic dye, methyl blue (MB, molecular formula: $C_{37}H_{27}N_3Na_2O_9S_3$, supplier: Tianjin Chemical Reagent Co. Ltd of China), was served as the target organic pollutant for photocatalytic experiments. The typical photocatalytic test was performed at room temperature, and 10 mg photocatalyst was added into 30 mL MB aqueous solution (40 mg/L). The solution was stirred in complete darkness at least for 3 h to achieve the equilibrium absorption of MB. Then the suspension was exposed to UV–Vis light irradiation using a 20 W low pressure mercury lamp which has spectral energy distribution centered at 365, 405, 436, 547, and 578 nm. After a regular interval, 2 mL of suspension was taken from the reaction vessels. The catalyst was separated by centrifugation and the reaction mixture was analyzed by UV/Vis spectrophotometer (U-4100, HITACHI).

Results and discussion

Figure 1 shows SEM and TEM images of the synthesized sample at 150 °C for 24 h. It is found that TiO_2 synthesized by the solvothermal process are sea-urchin-like 3D hierarchical microspheres assembled by numerous 1D nanoneedles. The 3D hierarchical microspheres are uniform with diameters about 2.5–3.0 μm. The diameter of nanoneedles is about 20–40 nm according to the high-resolution TEM image as shown in Fig. 1c. Furthermore, from the crashed microspheres in Fig. 1d we can find that the nanoneedles grow radially from the core of microspheres. It is difficult to clarify the preferred growth planes of nanoneedles in the core of microspheres because of the

overlap of nanoneedles. The HRTEM image of tip of nanoneedles in Fig. 1e evidences the single crystalline nature of nanoneedles. The distance between the adjacent lattice fringes (~0.32 nm) can be assigned to the interplanar distance of rutile TiO_2 (110). So the nanoneedles are grown along the rutile (110) crystal plane with a preferred orientation in the [001] direction. The EDS analysis in Fig. 1f shows that the 3D hierarchical microspheres are composed of Ti and O elements. No other extraneous metal elements are detected. (The signals of Cu and C are from the copper grid used.)

Figure 2 shows SEM images of samples obtained at various solvothermal temperatures. It is found that the morphology of samples depends on solvothermal temperatures. At 90 °C, the non-hierarchical TiO_2 microspheres are formed (Fig. 2a, b) and the diameters of them are about 2.0–5.0 μm. Although the surface of the microspheres is rough, no nanoneedles can be observed. The corresponding XRD pattern as shown in Fig. 3a indicates that the 90 °C-prepared TiO_2 microspheres are composed of rutile and traces of anatase phases. When the solvothermal temperature is increased to 120 °C, uniform sea-urchin-like 3D hierarchical microspheres with diameters of 3.0–4.0 μm are obtained (Fig. 2c, d). Numerous 1D nanoneedles can be seen on the surface of these microspheres. However, most of nanoneedles are not separated. The XRD pattern in Fig. 3b shows that the 120 °C-prepared hierarchical TiO_2 microspheres are also mixture made of rutile and a small amount of anatase, but the crystallization level is improved compared with that of 90 °C-prepared TiO_2 microspheres according to the increased XRD peak intensity. When the solvothermal temperature is increased to 150 °C, the perfect urchin-like 3D hierarchical microspheres, which consist of well-organized independent nanoneedles, are obtained (Fig. 2e, f). The diameter of microspheres is decreased to 2.5–3.0 μm and the diameter of nanoneedles is about 30 nm. The corresponding XRD pattern in Fig. 3c shows that the 150 °C-prepared hierarchical TiO_2 microspheres possess rutile phase only. When the solvothermal reaction is further elevated to 180 °C, the obtained TiO_2 microspheres exhibit the same 3D hierarchical morphology as that of 150 °C-prepared ones, but the microspheres became smaller (about 1.5 μm) and more uniform (Fig. 2g, h). Also, only diffraction peaks corresponding to the reflection of rutile phase are observed in the 180 °C-prepared TiO_2 microspheres (Fig. 3d) and the crystallization level is further improved compared with that of 150 °C-prepared ones. It is obviously concluded based on the experiments above that the solvothermal temperature has a significant influence on the hierarchical morphology, size, and crystal phase of TiO_2. In the present method, the well-defined urchin-like 3D hierarchical TiO_2 can be obtained when the temperature is higher than 120 °C. At the same time, the size of 3D hierarchical TiO_2 microspheres decreases with the increase of solvothermal

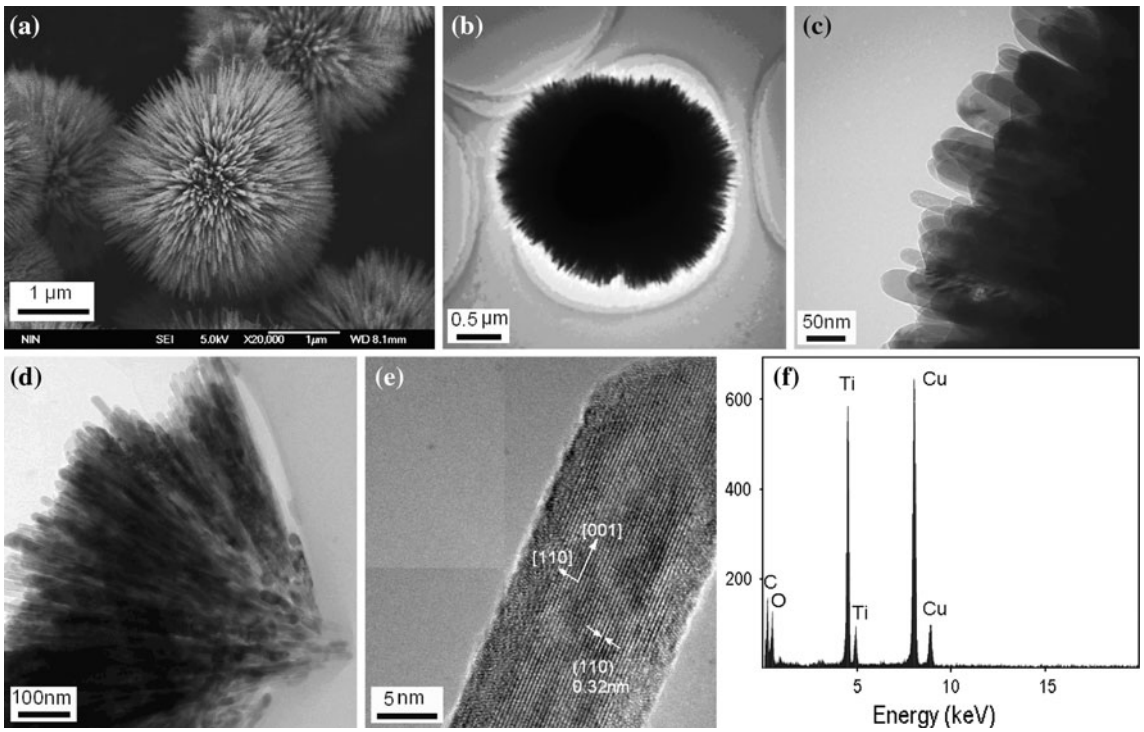

Fig. 1 SEM image (**a**), TEM images (**b**–**e**), and EDS (**f**) of the urchin-like hierarchical TiO_2

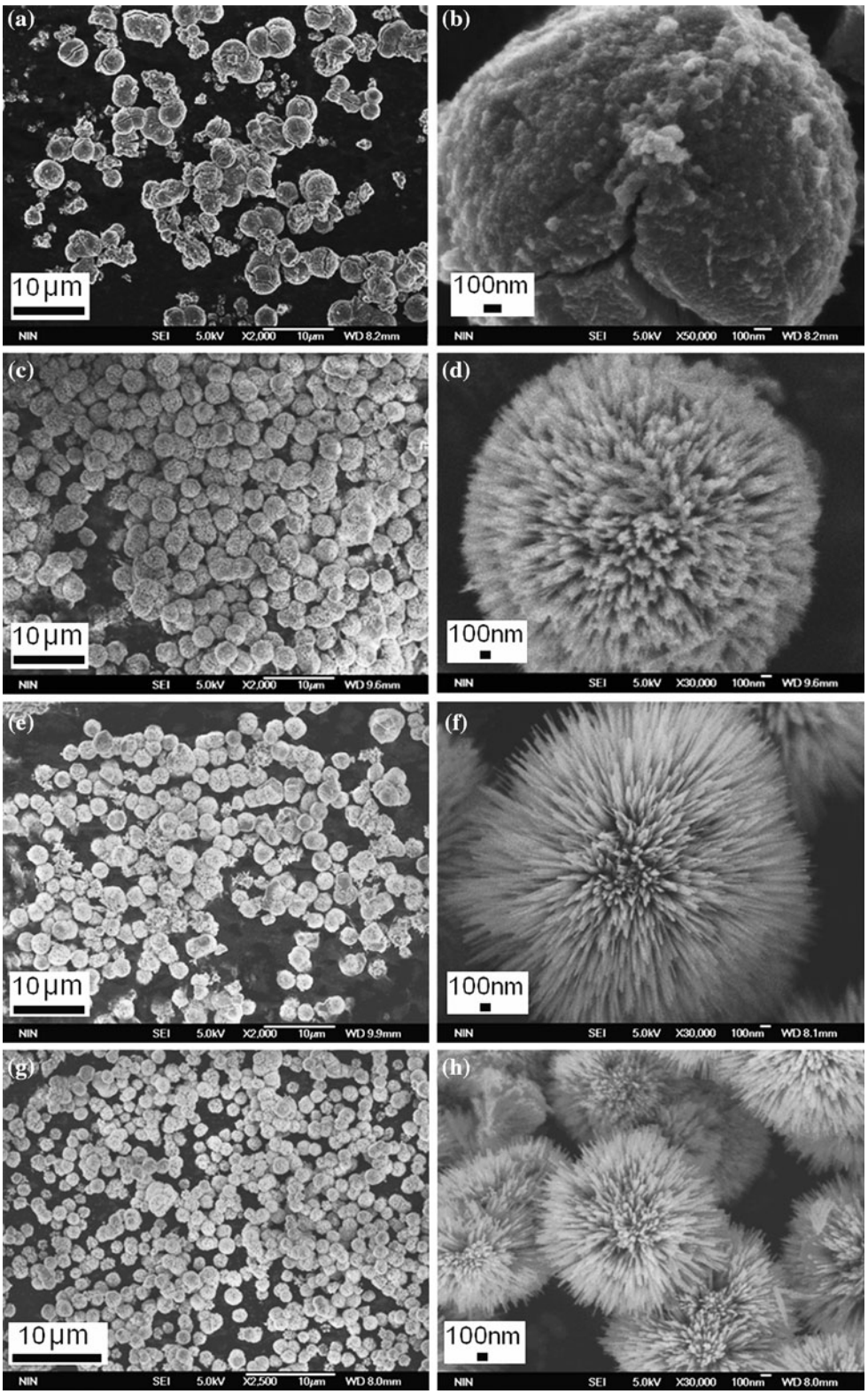

Fig. 2 SEM images of TiO_2 synthesized at various solvothermal temperatures: **a**, **b** 90 °C; **c**, **d** 120 °C; **e**, **f** 150 °C; **g**, **h** 180 °C

temperature but the crystallization level increases with the increase of solvothermal temperature. This may be attributed to the fact that high solvothermal temperature promotes the number of nucleation and the crystal growth.

Figure 4 shows the morphology change of TiO_2 with the precursor ratio of TBT to $TiCl_4$ when other experimental conditions, such as solvothermal temperature (150 °C), reaction time (24 h), and solvent volume (30 mL), are

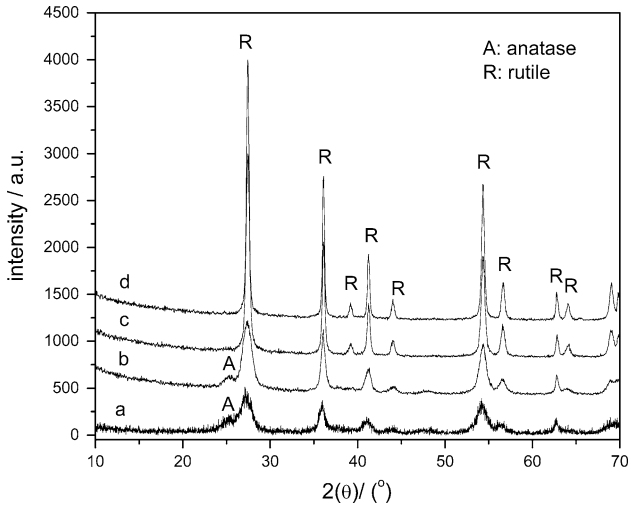

Fig. 3 XRD patterns of TiO_2 synthesized at various solvothermal temperatures: (*a*) 90 °C, (*b*) 120 °C, (*c*) 150 °C, (*d*) 180 °C

fixed. The concentration of $TiCl_4$ solution used for preparing the sample (a), (b), (c), and (d) is 50 wt%, and that used for sample (e) is 25 wt%. It is found that, when the mole ratio of TBT to $TiCl_4$ is 1:0.44, only irregular particles are obtained and no 3D hierarchical microspheres are formed (Fig. 4a). When the ratio of TBT to $TiCl_4$ is 1:0.65 and 1:1.30, the TiO_2 with perfect 3D micro/nanohierarchical morphology is prepared (Fig. 4b, c). When the ratio is decreased to 1:2.61, however, only pure TiO_2 nanowires with large diameter of ~100 nm are formed and no 3D hierarchical microspheres are observed (Fig. 4d). Therefore, a proper precursor ratio of TBT to $TiCl_4$ solution is necessary for the formation of well-defined urchin-like 3D hierarchical TiO_2. Furthermore, when the concentration of $TiCl_4$ solution is 25 wt% and the ratio of TBT to $TiCl_4$ is still remained to be 1:0.65, 3D micro/nanohierarchical microspheres with the diameters about 1.0 μm are formed as shown in Fig. 4e. This possibly provides an effective way to adjust the size of 3D micro/nanohierarchical microspheres by controlling the concentration of $TiCl_4$ solution. It was reported that the concentration of HCl and the water content in solution were two important factors to the morphology and crystal phase of TiO_2 [38, 39]. Therefore, the dependence of morphology on the ratio of TBT to $TiCl_4$ may be also related to the change of HCl concentration and water content because the $TiCl_4$ aqueous solution is used in the present experiment. In this $TiCl_4$ aqueous solution, there is not only water but also HCl that is produced by decomposition of $TiCl_4$. Thus, when the mole ratio of TBT to $TiCl_4$ is 1:0.44, the HCl concentration is low and as a result irregular aggregated TiO_2 particles as shown in Fig. 4a are easily obtained due to rapid hydrolysis of TBT and no 3D hierarchical microspheres are formed. When the ratio is decreased to 1:2.61, however, the HCl concentration is too high to induce the initial formation of TiO_2 microspheres and thus only pure TiO_2 nanowires as shown in Fig. 4d are grown under solvothermal reaction.

In addition, to understand the formation mechanism of urchin-like 3D hierarchical TiO_2, we also investigated the corresponding time-dependent evolution of morphology and crystal structure of samples. Figure 5 shows SEM images of samples after different reaction times at 150 °C. As shown in Fig. 5a, the sample obtained at 150 °C for 1 h is irregular aggregates consisting of small nanoparticles with diameters of ~30 nm (Fig. 5b). After solvothermal reaction for 2 h at 150 °C, the microspheres with an average diameter about 2.0 μm are formed (Fig. 5c). The high-resolution SEM image in Fig. 5d further confirms the microspheres are waxberry-like, but some separated nanoparticles are still observed. After solvothermal reaction for 4 h at 150 °C, however, the morphology of the microspheres changes obviously. Not only the diameter of microspheres is increased to 3.0–4.0 μm but also the surface becomes very rough and irregular. It is observed that a few nanoneedles appear on the surface of microspheres and some microspheres start to become sea-urchin-like. As the reaction time increases to 8 h, the morphology of the sample is still similar to the one that subjected to solvothermal reaction for 4 h. When the reaction is carried out for 12 h, most of microspheres start to show clearly sea-urchin-like 3D hierarchical morphology as shown in Fig. 5g, but some intermediate structures (i.e., nanoneedles with different length disperse randomly on the microsphere surface) are still observed as shown in Fig. 5h. After solvothermal reaction for 16 h at 150 °C, well-organized sea-urchin-like 3D hierarchical TiO_2 is formed and the morphology shows less changes even if the reaction time is further increased. According to the time-dependent evolution of morphology, we can find that the nonhierarchical TiO_2 microspheres have been formed in the initial stage of reaction. As the reaction time increases, the nonhierarchical TiO_2 microspheres gradually transform into the urchin-like hierarchical structure. This indicates that the formation of urchin-like micro/nanohierarchical structure may not follow a 'growth-then-assembly' process reported by the other study [33]. The corresponding time-dependent evolution of crystal phase of samples is also recorded by the XRD patterns in Fig. 6. It is worthy to note that all samples obtained at 150 °C within 1–12 h are made of rutile and a small amount of anatase, while the intensity of diffraction peaks corresponding to the reflections of rutile increases with the increase of reaction time. When the sample subjected to solvothermal reaction for 16 h at 150 °C, however, only the diffraction peaks of rutile are observed. The crystal structure shows less change when the reaction time is further increased. It indicates that the transformation from nonhierarchical TiO_2 microspheres to the urchin-like

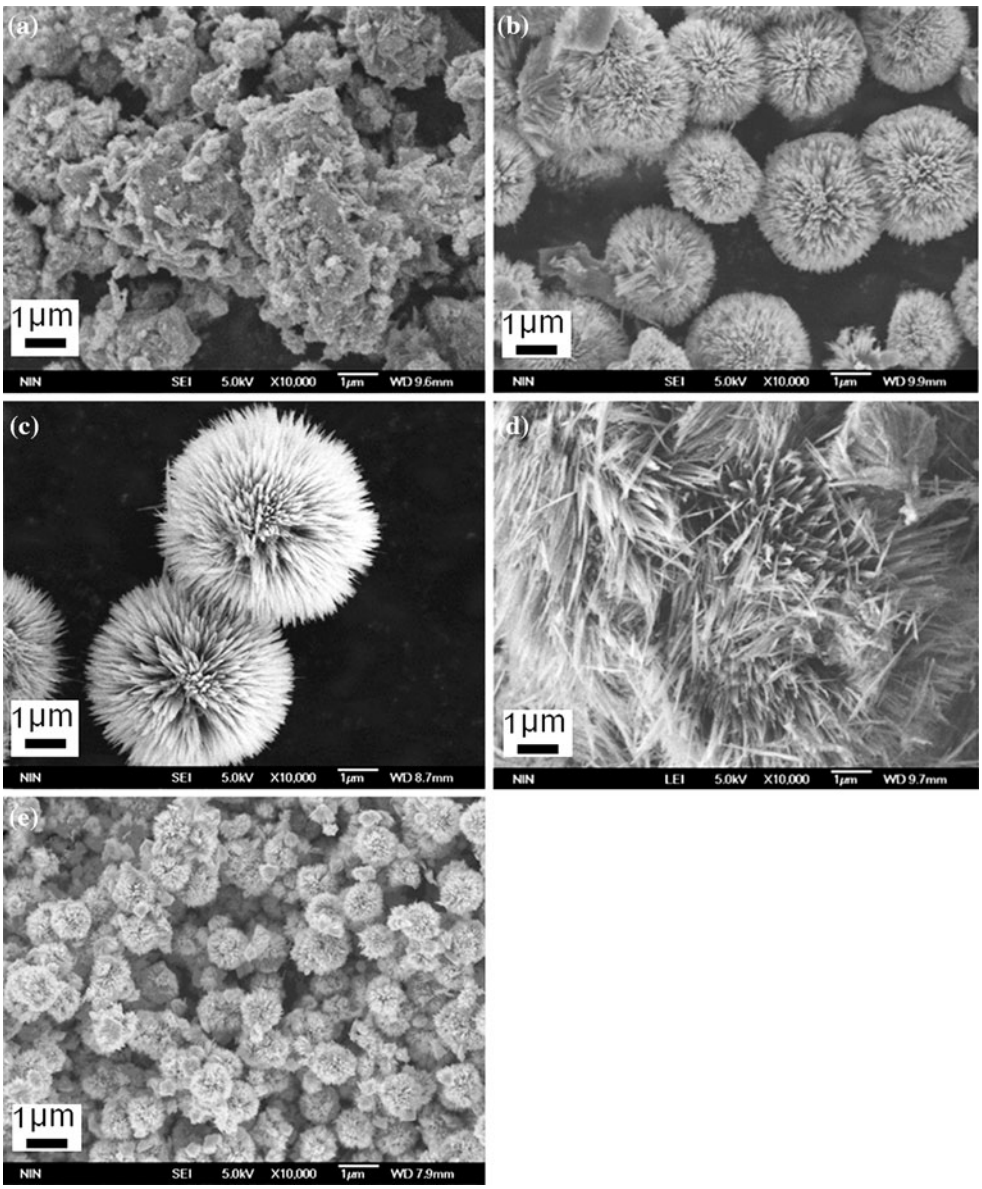

Fig. 4 SEM images of TiO_2 synthesized at the different mole ratio of TBT to $TiCl_4$. **a** TBT:$TiCl_4$ = 1:0.44; **b** TBT:$TiCl_4$ = 1:0.65; **c** TBT:$TiCl_4$ = 1:1.30; **d** TBT:$TiCl_4$ = 1:2.61; **e** TBT:$TiCl_4$ = 1:0.65. ($TiCl_4$ aqueous solution used in samples **a**, **b**, **c**, and **d** is 50 wt%, but 25 wt% used in sample **e**)

hierarchical TiO_2 microspheres has finished, which is in accordance with the time-dependent evolution of morphology. Therefore, combining the time-dependent evolution of morphology with crystal phase of samples, we can conclude that the nonhierarchical TiO_2 microspheres composed of nanocrysal are firstly formed in the initial stage of reaction. Then, the nonhierarchical TiO_2 microspheres gradually transform into the urchin-like hierarchical structure followed by crystallization process. This crystallization process may be very important to the evolution of TiO_2 morphology. We will discuss it in the next section.

It was generally popular to explain the formation of 3D hierarchical structure with a two-stage growth mechanism involving the initial formation of primary 1D nanostructure and subsequently self-assembly, i.e., a 'growth-assembly' process [33]. However, our experimental results show that there must be another mechanism which is responsible for the formation of sea-urchin-like 3D hierarchical TiO_2. According to the time-dependent evolution of morphology (Fig. 5) and the crystal structure (Fig. 6), we propose a new growth process as depicted in Fig. 7. At the initial stage of reaction, a large number of TiO_2 nanoparticles as shown in Fig. 7a are firstly formed, and then the nanoparticles

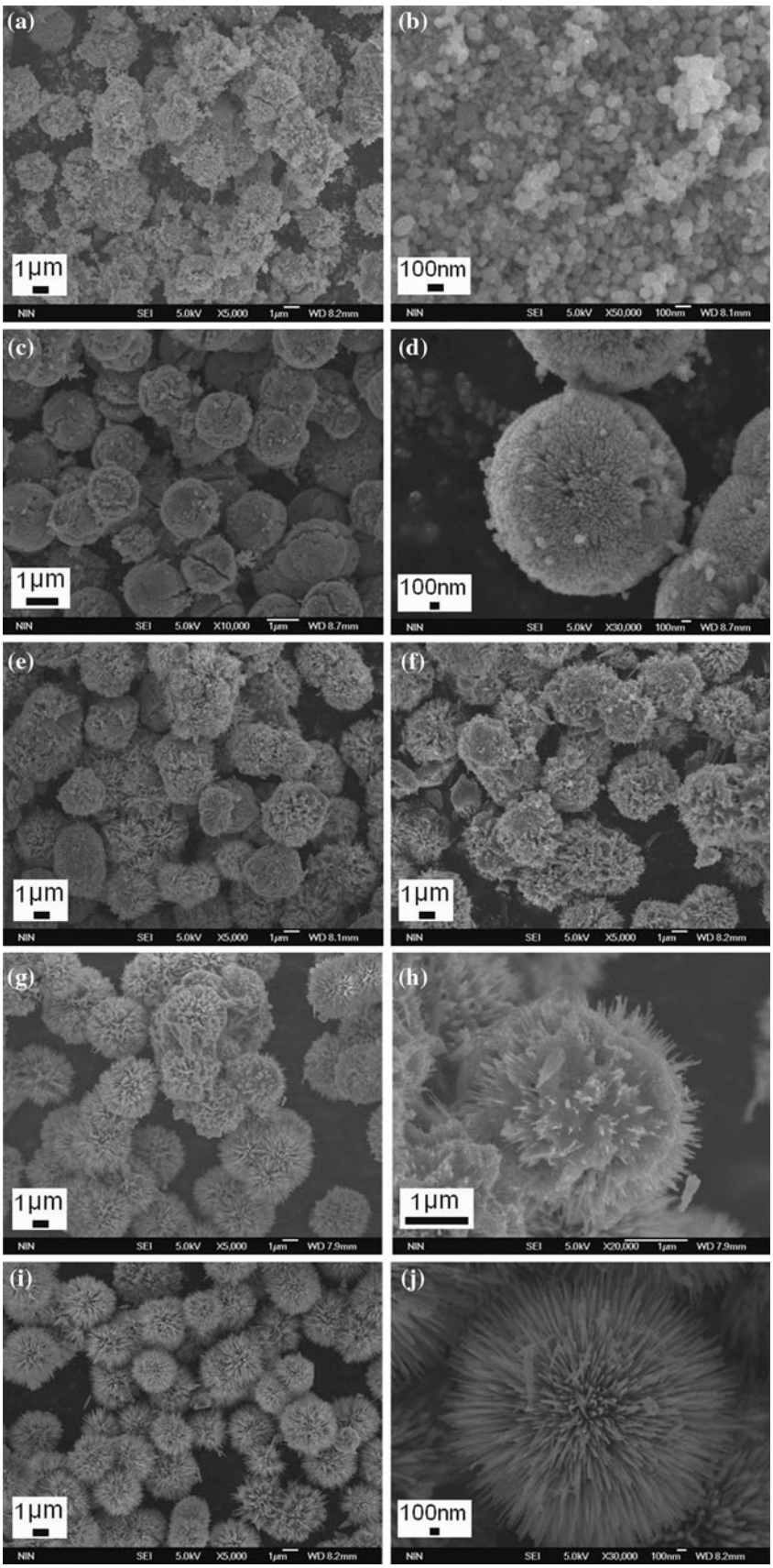

Fig. 5 SEM images of TiO_2 synthesized after different reaction time: **a**, **b** 1 h; **c**, **d** 2 h; **e** 4 h; **f** 8 h; **g**, **h** 12 h; **i**, **j** 16 h

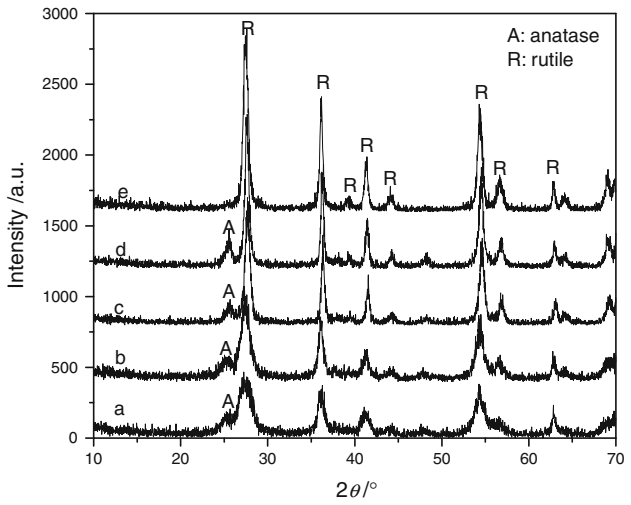

Fig. 6 XRD patterns of TiO_2 synthesized after different reaction time: (*a*) 1 h, (*b*) 4 h, (*c*) 8 h, (*d*) 12 h, (*e*) 16 h

aggregate into nonhierarchical microspheres (Fig. 7b). This process is called nucleation and self-assembly. In this stage, the precursor ratio of TBT to $TiCl_4$ and the concentration of $TiCl_4$ solution are two important factors to the shape and size of samples according to Fig. 4. As the reaction time increases, the small nanocrystal and amorphous TiO_2 nanoparticles are dissolved and recrystallized to gradually form rutile TiO_2 nanoneedles on the surface of microspheres (Fig. 7c, d) in order to maintain a more stable thermodynamics state. This process is called dissolution and recrystallization [40]. In this stage, the solvothermal temperature is an important factor to the formation of urchin-like hierarchical microspheres according to Fig. 2. When the solvothermal temperature is too low, the dissolution and recrystallization process will not be carried out and the resulted sample is nonhierarchical microspheres as shown in Fig. 2a.

Finally, the photocatalytic activity of urchin-like hierarchical TiO_2 with different sizes is measured and compared with P25 by photodegradation of MB as the model reaction under UV–Vis light. Figure 8 shows the typical absorbance spectra of MB solution as a function of irradiation time when urchin-like hierarchical TiO_2 with mean diameter of $\sim$1.0 μm is used as photocatalyst. It is found that the absorbing intensity of MB decreases with the irradiation time, indicating the rapid photodegradation of MB. Figure 9 compares the change of normalized temporal concentration (C/C_0) of MB during photodegradation by urchin-like hierarchical TiO_2 with different diameters and P25 on the basis of equal mass of photocatalyst. Here, the C/C_0 is proportional to the normalized maximum absorbance (A/A_0) and derives from the change in the dye's absorption peak ($\lambda = 590$ nm). It is found that the photocatalytic degradation efficiency follows the order: TiO_2 ($\sim$1.0 μm) > TiO_2 ($\sim$2.0 μm) > P25 > TiO_2 ($\sim$3.0 μm). The photocatalytic activity of urchin-like hierarchical TiO_2 ($\sim$1.0 μm) and TiO_2 ($\sim$2.0 μm) are more efficient than that of well-recognized P25 photocatalyst. According to the N_2 adsorption–desorption isotherm, the special surface area (S_{BET}) of P25 is 53 m^2/g, which is slightly higher than that ($S_{BET,\ 1.0\ \mu m} = 41\ m^2/g$, $S_{BET,\ 2.0\ \mu m} = 35\ m^2/g$, $S_{BET,\ 3.0\ \mu m} = 37\ m^2/g$) of urchin-like hierarchical TiO_2. On the basis of equal surface area of photocatalyst, we also investigate the photocatalytic degradation efficiency of different TiO_2. It is also found that all urchin-like hierarchical TiO_2 have higher photocatalytic efficiency compared to P25. We assume that this may be attributed to the unique micro/nanohierarchical structure of TiO_2 because it has been proposed that the micro/nanohierarchical microspheres could

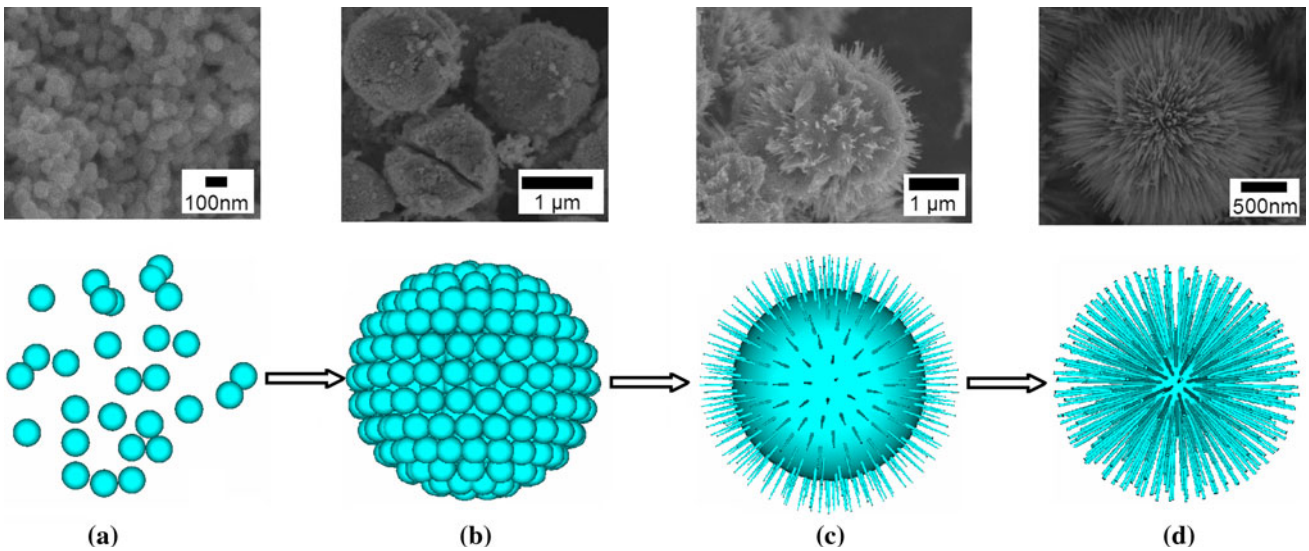

Fig. 7 Schematic illustration of the formation process of 3D urchin-like hierarchical TiO_2

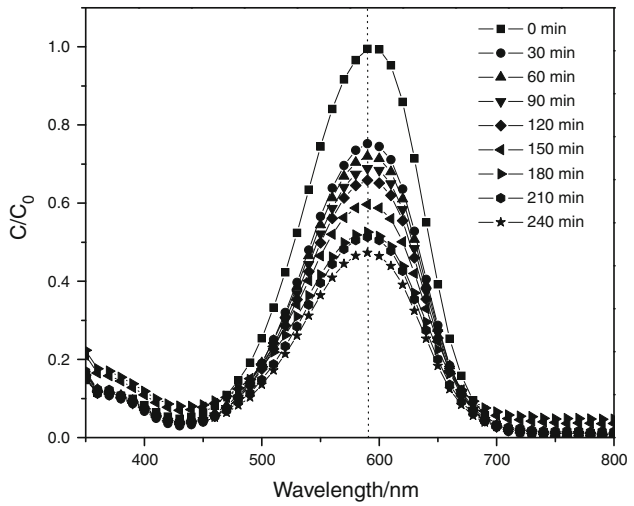

Fig. 8 The absorbance spectra of methyl blue as a function of irradiation time when urchin-like hierarchical TiO_2 with mean diameter of ~1.0 μm is used as photocatalyst

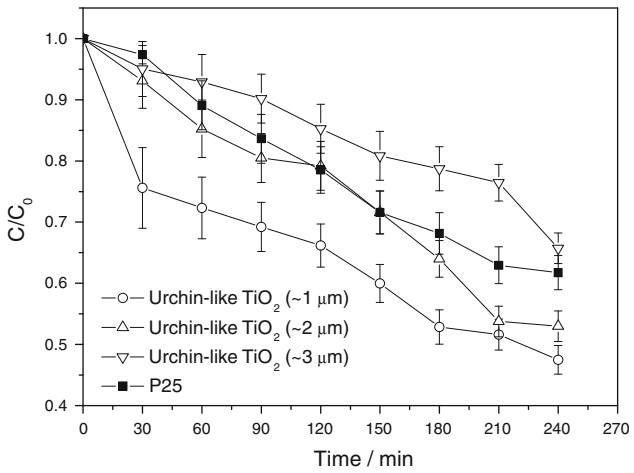

Fig. 9 Photodegradation of methyl blue for P25 and urchin-like TiO_2 with different diameters under UV–Vis light

absorb more incidental light through multiple-reflection of hierarchical microspheres [24]. For urchin-like hierarchical TiO_2 microspheres, the photocatalytic performance decreases with the increase of diameter of microspheres. In addition, another advantage of the urchin-like hierarchical TiO_2 over P25 is that it is easy to separate the urchin-like hierarchical TiO_2 from MB solution by filtration or sedimentation method after photocatalytic reaction due to its microsize.

Conclusions

Well-organized 3D urchin-like hierarchical TiO_2 microspheres with various diameters (1–4 μm) were prepared successfully. The morphology and size of TiO_2 microspheres could be effectively controlled by adjusting the precursor ratio of TBT to $TiCl_4$, the concentration of $TiCl_4$ solution, the solvothermal temperature, and the reaction time. Based on the observation of the morphology and crystal structure of diameters as a function of the reaction time, a new mechanism including nucleation, self-assembly, dissolution and recrystallization processes was proposed to explain the formation of urchin-like hierarchical TiO_2. Photodegradation experiments showed that the urchin-like TiO_2 exhibited higher photocatalytic activity compared to the commercial P25. The results may be useful for the design and preparation of hierarchical TiO_2 microspheres with enhanced properties.

Acknowledgements This work was supported by the National Natural Science Foundation of China (No. 60778042 and No. 50602036) and NPU Foundation for Fundamental Research (No. JC201159).

References

1. Liu G, Wang L, Yang HG, Cheng HM, Lu GQ (2010) J Mater Chem 20:831
2. Manso M, Ogueta S, García P, Pérez-Rigueiro J, Jiménez C, Martínez-Duart JM, Langlet M (2002) Biomaterials 23:349
3. Montazer M, Pakdel E, Behzadnia A (2011) J Appl Polym Sci 121:3407
4. Kong H, Song J, Jang J (2010) Environ Sci Technol 44:5672
5. Hwang SH, Kim C, Jang J (2011) Catal Commun 12:1307
6. Kim YJ, Lee MH, Kim HJ, Lim G, Choi YS, Park NG, Kim K, Lee WI (2009) Adv Mater 21:3668
7. Thiel J, Pakstis L, Buzby S, Raffi M, Ni C, Pochan DJ, Ismat SS (2007) Small 3:799
8. Zhao XP, Yin JB (2002) Chem Mater 14:2258
9. Wang BX, Zhao XP (2005) Adv Funct Mater 15:1815
10. Xiang LQ, Zhao XP (2006) J Colloid Interface Sci 296:131
11. Whitesides GM, Grzybowski B (2002) Science 295:2418
12. Sau TK, Rogach AL (2010) Adv Mater 22:1781
13. Yin JB, Xiang LQ, Zhao XP (2007) Appl Phys Lett 90:113112
14. Hanaor DAH, Sorrell CC (2011) J Mater Sci 46:855. doi:10.1007/s10853-010-5113-0
15. Tanaka S, Nogami D, Tsuda N, Miyake Y (2009) J Colloid Interface Sci 334:188
16. van der MT, Mattson A, Oesterlund L (2007) J Catal 25:131
17. Bian ZF, Zhu J, Cao FL, Huo YN, Lu YF, Li HX (2010) Chem Commun 46:8451
18. Kang XW, Chen SW (2010) J Mater Sci 45:2696. doi:10.1007/s10853-010-4254-5
19. Zhang J, Zhao DS, Wang JL, Yang LY (2009) J Mater Sci 44:3112. doi:10.1007/s10853-009-3413-z
20. Yu HK, Eun TH, Yi GR, Yang SM (2007) J Colloid Interface Sci 316:175
21. Hongo T, Yamazaki A (2010) J Mater Sci 45:275. doi:10.1007/s10853-009-3980-z
22. Yogi C, Kojima K, Takai T, Wada N (2009) J Mater Sci 44:821. doi:10.1007/s10853-008-3151-7
23. Coutinho CA, Gupta VK (2009) J Colloid Interface Sci 333:457
24. Zhao Y, Jiang L (2009) Adv Mater 21:3621
25. Bartl MH, Boettcher SW, Frindell KL, Stucky GD (2005) Acc Chem Res 38:263

26. O'Dwyer C, Navas D, Lavayen V, Benavente E, Santa Ana MA, Gonzalez G, Newcomb SB, Sotomayor Torres CM (2006) Chem Mater 18:3016
27. Yin JB, Zhao XP, Xiang LQ, Xia X, Zhang ZS (2009) Soft Matter 5:4687
28. Seisenbaeva GA, Moloney MP, Tekoriute R, Tekoriute R, Hardy-Dessources A, Nedelec JM, Gun'ko YK, Kessler VG (2010) Langmuir 26:9809
29. Wang C, Yin L, Zhang L, Qi Y, Lun N, Liu N (2010) Langmuir 26:12841
30. Yang S, Gao L (2006) Mater Chem Phys 99:437
31. Li H, Bian Z, Zhu J, Zhang D, Li G, Huo Y, Li H, Lu Y (2007) J Am Chem Soc 129:8406
32. Cheng QL, Pavlinek V, He Y, Li CZ, Saha P (2011) Colloid Polym Sci 289:799
33. Mao YB, Kanungo M, Hemraj-Benny T, Wong SS (2006) J Phys Chem B 110:702
34. Zhang D, Li G, Wang F, Yu JC (2010) CrystEngComm 12:1759
35. Liu G, Yang HG, Sun C, Cheng L, Wang L, Lu GQ, Cheng HM (2009) CrystEngComm 11:2677
36. Wei J, Yao J, Zhang X, Zhu W, Wang H, Rhodes MJ (2007) Mater Lett 61:4610
37. Bai X, Xie B, Pan N, Wang X, Wang H (2008) J Solid State Chem 181:450
38. Lee JH, Yang YS (2005) Mater Chem Phys 93:237
39. Park HK, Kim DK, Kim CH (1997) J Am Ceram Soc 80:743
40. Wu JM, Hayakawa S, Tsuru K, Osaka A (2002) Scr Mater 46:705